



Biosorption performances of raw and chemically modified biomasses from *Perenniporia subacida* for heterocycle dye Neutral Red

Jing Si¹, Bao-Kai Cui¹, Yuan Yuan, Yu-Cheng Dai*

Institute of Microbiology, Beijing Forestry University, P.O. Box 61, No. 35 Tsinghua East Road, Haidian District, Beijing 100083, P.R. China, Tel./Fax: +86 10 62336309; emails: jingsi1788@126.com (J. Si), cuibaokai@yahoo.com (B.-K. Cui), 1018yy@sina.com (Y. Yuan), daiyucheng2013@gmail.com (Y.-C. Dai)

Received 5 November 2014; Accepted 6 February 2015

ABSTRACT

Biosorption performances of raw and chemically modified biomasses (treated with (i) lipid removal, (ii) phosphate esterification, (iii) amine methylation, and (iv) amine propylamination) from white rot fungus *Perenniporia subacida* were investigated for heterocycle dye Neutral Red removal. Better dye uptake was obtained at constant temperature and agitation speed with the optimum variables like initial pH at 3.0, initial dye concentration at 50 mg/L, surfactant Tween 80 at 2.5% (V/V), inorganic salt NaCl at 0.1 M, and first 60 min of reaction time. A comparison of the different isotherm models indicated that the biosorption process by the fungal biomass followed the Langmuir isotherm model. The kinetic data could be well described by the pseudo-second-order model. Calculated thermodynamic parameters of biosorption indicated the exothermic and spontaneous process. Additionally, the modification of biomass with amine propylamination increased the biosorption capability of Neutral Red dye about 1.36-fold of the raw fungal biomass. These observations were characterized by FT-IR, SEM, and X-ray diffraction, respectively.

Keywords: *Perenniporia subacida* biomass; Biosorption; Chemical modification; Isotherms; Kinetics

1. Introduction

Extensive use of synthetic dyes in many industrial processes such as textile, paint, solvent, paper, pulp, printing, food and cosmetic results in large quantities of colored effluents [1]. Over a hundred thousand commercially available dyes exist and more than 7×10^5 tons are produced annually [2]. Consequently, large quantities of dyes are emitted into effluents from various industries, for example, the textile and food industries [3]. Contamination of water sources with

synthetic dyes as a consequence of various industrial activities has become a serious problem. Discharge of dye-contaminated wastewaters into aquatic environment without treatment can lead to adverse effects on the esthetic quality of water bodies and impact the ecosystem by reducing the sunlight penetration and gas solubility in water [4]. Moreover, some dyes as well as their breakdown products are highly toxic and potentially carcinogenic, mutagenic, or allergenic to aquatic life. Therefore, treatment of dye-contaminated aquatic systems and improvement of water quality are important topics in the field of environmental

*Corresponding author.

¹These authors contributed equally to this work and shared the first author.

technologies [5]. The traditional methods for color removal, including photooxidation, electrocoagulation, adsorption, reverse osmosis, membrane filtration, flocculation, oxidation (ozonation, hydrogen peroxide, and chlorine), deep-well injection, ionic exchange, incineration, solvent extraction, Fenton agents and irradiation, are limited because of the excessive usage of chemicals, accumulation of concentrated sludge, expensive plant requirements, and high operational costs [6].

Biosorption is found to be an alternative low cost and eco-friendly technology based on the biomaterial–pollutant interaction. As sometimes the tested sorbent materials do not possess good biosorption capabilities or need long biosorption equilibrium times, there is a need to search for more effective adsorbents. Activated carbon has been widely utilized as an adsorbent for the removal of textile dyes from wastewater. However, this technique is ineffective due to its cost and poor regeneration [7]. Low-cost materials have also been extensively studied as alternative adsorbents for dyes, recent studies showed that waste biomasses, shells, rice husk ashes, and fungi can be used as effective adsorbents in biosorption [4,8,9].

White rot fungi have been proved to possess high dye binding capabilities due to the presence of polysaccharides, proteins, or lipid on the cell wall surface containing various functional groups such as amino, hydroxyl, carboxyl, phosphate, and sulfate, which can act as binding sites for dye molecules [10,11]. The efficiency of the biosorption process depends on various factors including the type of biomass, solution pH, temperature, and the type of pollutant [11]. One method for improving the biosorption capacities of adsorbents is through modification of biomass using various chemical agents, or by oven heating or autoclaving, or by genetic modification of the cells to change their biosorption properties [12]. Moreover, current researches demonstrate that different kinds of biomaterials interact with dye molecules, chlorides, heavy metals, and other organic substances and they successfully remove these contaminants from aqueous media [3,13,14].

Perenniporia subacida is a common white rot fungus in China [15], and it is also recorded as a forest pathogen [16] and medicinal fungus [17]. Recent study showed it has the ability to decolorize several kinds of dyes including Neutral Red, Congo Red, Methylene Blue, and Chromazurine [18]. In this work, the biomass prepared from *P. subacida* was chemically modified by lipid removal (LR), phosphate esterification (PE), amine methylation (AM), and amine propylation (AP) in order to prepare a novel, effective, and alternative material for uptake of heterocycle dye Neu-

tral Red. The biosorption properties of the modified biomasses were explored as a function of batch operating conditions including pH, initial dye concentration, surfactant, ionic strength, and reaction time. Isotherm and kinetic analysis of the biosorption process was performed in terms of the Langmuir, Freundlich, and Temkin isotherm models, as well as the pseudo-first-order, pseudo-second-order, and intraparticle diffusion kinetic models. Additionally, Fourier transform infrared spectroscopy (FT-IR), scanning electron microscope (SEM), and X-ray diffraction (XRD) were employed to evaluate the possible dye–biosorbent interactions.

2. Materials and methods

2.1. Chemical reagents and adsorbate

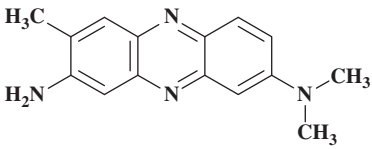
Table 1 presents the heterocycle dye Neutral Red used in this study and its color index number, chemical class, and wavelength. A stock solution (1,000 mg/L) of the dye was prepared by dissolving an approximate amount of it in deionized water and being filtered through a 0.22- μ m membrane to remove bacteria. The solutions for all experiments were prepared through dilutions of stock solution. The desired solution pH was adjusted with diluted 1 M NaOH and 1 M HCl. All the reagents used were of analytical grade.

2.2. Fungal strain and raw biomass preparation

P. subacida IFP 003942 was isolated from Changbai Mountain of Jilin Province in China. This strain was maintained through periodic (monthly) transfer on yeast extract glucose agar (YGA) at 4°C. The YGA medium used for the experiment contained (g/L of distilled water): yeast extract 5.0, glucose 20.0, agar 20.0, KH_2PO_4 1.0, $\text{MgSO}_4 \cdot 7\text{H}_2\text{O}$ 0.5, $\text{ZnSO}_4 \cdot 7\text{H}_2\text{O}$ 0.05 and vitamin B1 0.01, and the pH value of the medium was adjusted to 5.0 before sterilization. Prior to use, the stored fungal strain was activated in 100 mL of yeast extract glucose medium (YG, identical to YGA without agar) and cultured on a rotary shaker at 28°C with a speed of 150 rpm. After six days, mycelia were homogenized using an Ace Homogenizer (Hengao Co., Tianjin, China) at 5,000 rpm for 30 s, and the pellet suspensions were later prepared as inocula for the next experiment.

An aliquot of 10 mL of inocula (0.087 g, dry weight) was inoculated into a 250-mL Erlenmeyer flask containing 100 mL of YG medium, and incubated at 28°C and 150 rpm. After five days, the cells were

Table 1
Characteristics of heterocycle dye Neutral Red used in the present study

Chemical structure	
Color index number	50040
Color index name	Basic Red 5
Chromophore	Heterocycle
Molecular weight (g/mol)	288.78
Wavelength (nm)	553

then harvested by filtration, rinsed several times with generous amounts of deionized water, and then oven-dried at 75°C to constant weight. For the biosorption studies, the raw biomass was ground to powder in a disintegrator and sieved through a 75 µm ASTM Standard sieve to obtain uniform particle size.

2.3. Chemical modification of raw biomass

2.3.1. Lipid removal

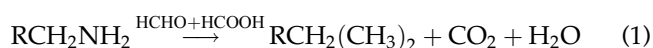
One gram of raw biomass was added to 75 mL of acetone in a 250-mL Erlenmeyer flask. The reaction mixture was agitated on a rotary shaker for 6 h with a shaking speed of 150 rpm at 50°C, and then kept without shaking for 24 h. This treatment results in the removal of surface lipids of fungal biomass. Afterward, the biomass was washed several times with deionized water and oven-dried at 75°C to constant weight.

2.3.2. Phosphate esterification

Forty milliliters of triethyl phosphate and 30 mL of nitromethane were added to 1.0 g of raw biomass in a 250-mL Erlenmeyer flask and the reaction mixture was shaken on a rotary shaker for 6 h with agitation speed of 150 rpm at 50°C. Afterward, the biomass was washed several times with deionized water and oven-dried at 75°C to constant weight.

2.3.3. Amine methylation

Another aliquot of 1.0 g of raw biomass was inoculated into a 250-mL Erlenmeyer flask containing 20 mL of pure methanal and 40 mL of methanoic acid. The reaction mixture was shaken on a rotary shaker for 6 h with agitation speed of 150 rpm at 50°C. This treatment results in methylation of amine and the general reaction scheme is:



Afterward, the chemically treated biomass was washed several times with deionized water and oven-dried at 75°C to constant weight.

2.3.4. Amine propylamination

Fifty milliliters of 0.1 M propylamine was added to 1.0 g of raw biomass in a 250-mL Erlenmeyer flask. The reaction mixture was shaken on a rotary shaker for 3 h with a speed of 150 rpm at 50°C; subsequently the biomass was washed several times with deionized water and oven-dried at 75°C to constant weight. The modification leads to the conversion of carboxylic acid groups to amine groups by the following reaction:



2.4. Batch biosorption studies

The bath dye biosorption experiments were conducted in a 250-mL Erlenmeyer flask containing 100 mL of dye solution. A weighed amount of 100 mg of raw or chemically modified biomasses was added to the dye solution. The reaction mixtures were shaken with agitation speed of 150 rpm at 28°C in the dark to avoid dye polymerization by light. The influences of pH (1.0–10.0), initial dye concentration (5–200 mg/L), surfactant (Polyoxyethylene sorbitol monooleate 80, Tween 80; 0.5–5.0%, V/V), ionic strength (NaCl, 0–1.0 M), and reaction time (0–80 min) were evaluated to optimize the impact factors for the dye biosorption by varying the factor under study and keeping other factors constant. The levels used were determined empirically. Uninoculated (without dry powders) flasks and inoculated (with fresh biomass)

flasks with media YGA addition were selected as controls under identical conditions. Experiments were all performed in triplicate and the results obtained were expressed in terms of means and standard error means.

Once the biosorption equilibrium was achieved, the mixtures were centrifuged at 12,000 rpm for 15 min and the pure (without dye biosorption experiment) and dye-loaded (after dye biosorption experiment) biomasses were oven-dried at 75°C to constant weight for FT-IR, SEM, and XRD analysis. The supernatant's UV-Visible spectra before and after dye biosorption were recorded between 200 and 800 nm with a UV-Visible spectrophotometer (UNICO 4802, Younike Co., Shanghai, China). The dye removal efficiency (%) and the amount of dye adsorbed on the biomass (q_e) were calculated by Eqs. (3) and (4) respectively as follows:

$$\text{Dye removal efficiency (\%)} = \frac{C_i - C_e}{C_i} \times 100 \quad (3)$$

$$q_e = \frac{V(C_i - C_e)}{m} \quad (4)$$

where C_i and C_e are the initial and equilibrium concentrations (mg/L) of heterocycle dye Neutral Red, q_e is the dye uptake (mg/g), V is the solution volume (L), and m is the mass of biomass (g).

Biosorption data were subject to equilibrium modeling to have a better understanding of mechanism of heterocycle dye biosorption using three parameter isotherms such as Langmuir, Freundlich, and Temkin. Kinetic rate constants were determined using pseudo-first-order, pseudo-second-order, and intraparticle diffusion models.

3. Results and discussion

3.1. Influences of impact factors on dye biosorption capability

3.1.1. Initial pH

In this study, the influence of initial pH on the biosorption of heterocycle dye Neutral Red onto untreated and treated biomasses was studied by varying pH from 1.0 to 10.0, while the initial dye concentration and reaction time were kept constant at 15 mg/L and 60 min, respectively. As shown in Fig. 1(a), lower biosorption capability was observed as the initial pH from 7.0 to 10.0 after 60 min. Dye uptake of Neutral Red displayed a typical bell-shaped pH profile, which exhibited stronger capability over a

broad pH range of 1.0–6.0, with an optimum pH at 3.0 for all the treated and untreated *P. subacida* biomasses. This result was consistent with the previous study [19] which showed lower pH was available for anionic dyes biosorption. Higher dye uptake obtained at relatively lower pH might be due to the electrostatic interaction between negatively charged dye molecules and positively charged fungal cell surface [20]. Since the peak value of Neutral Red dye biosorption for untreated and treated biomasses was detected at pH 3.0, further experiments were carried out at initial pH 3.0.

3.1.2. Initial dye concentration

Influences of various initial concentration of Neutral Red dye (5–200 mg/L) on the biosorption capabilities of raw and chemically modified biomasses from *P. subacida* are demonstrated in Fig. 1(b). Results showed that the uptake of dye at different concentrations of 5–50 mg/L gradually increased in the initial stages and then decreased as the reaction time until the equilibrium reached at the initial concentrations of 140 mg/L. Initial dye concentration provides an important driving force to overcome all mass transfer resistance of dye between the aqueous and solid phases [21]. Afterward, decline in dye removal may be due to the insufficient production of biomass for biosorption of higher concentrations of dyes [22].

The dye biosorption capability of AP-treated biomass was 53.64 mg/g after 60 min with the initial dye concentration at 50 mg/L, which was 1.15 times than that of raw biomass. With the increase in initial dye concentration, the biosorption capability of AP-treated biomass was dramatically increased compared to untreated or other treated biomasses. The higher dye removal of AP-treated biomass could be possibly attributed to the increase in amine functional groups on the biomass surface, demonstrating that this treatment stimulates the electrostatic force between the biomass and negatively charged dyes [23].

3.1.3. Surfactant Tween 80

It is well known that the surfactant has the capability to increase aqueous concentrations of low solubility compounds, thus leading to enhance their availability to micro-organisms. But in some cases, surfactant with higher concentrations has been reported to inhibit the biodegradation of organic compounds [24]. Thus, it is necessary to explore the influence of surfactant Tween 80 on the Neutral Red dye uptake of *P. subacida* biomass.

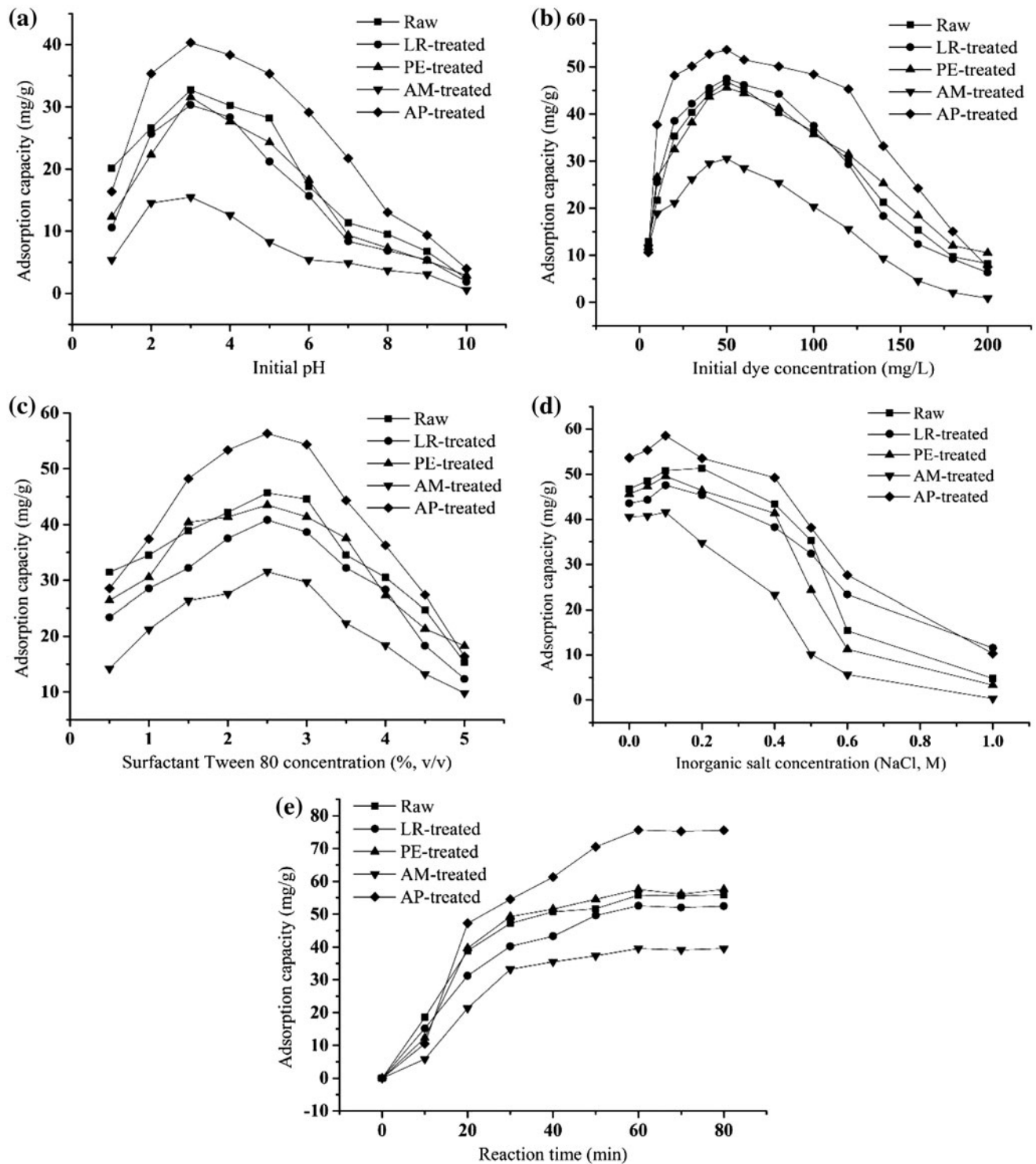


Fig. 1. Influences of (a) initial pH, (b) initial dye concentration, (c) surfactant Tween 80, (d) ionic strength, and (e) reaction time on the biosorption of heterocycle dye Neutral Red by raw and chemically modified biomasses from *P. subacida*. Chemically modification: LR, lipid removal; PE, phosphate esterification; AM, amine methylation; AP, amine propylation.

The plot of dye uptake vs. the concentration of Tween 80 is shown in Fig. 1(c). As can be seen from this figure, maximums of dye uptakes were obtained in the presence of Tween 80 with concentration at 2.5% (V/V) for raw and chemically modified biomasses, which were approximately 1.08-, 1.17-, 1.17-, 1.02-, and 1.18-fold, respectively, than those of all treatments without Tween 80 after 60 min, indicating that the surfactant at relatively lower concentrations could enhance the dye uptake by formation of micelles in the dye solution [25]. However, the dye removal was restrained with Tween 80 over a range of concentration from 3.5 to 5.0% (V/V). It was concluded that high concentration surfactant has an inhibitive effect on the dye biosorption capability of fungal biomass. Thereby, a suitable surfactant with a reasonable concentration is crucially important for retaining the high dye uptake of fungal biomass [26].

3.1.4. Ionic strength

High amounts of chlorides were generally used in dye bath to ensure the maximum fixation of dye to the cellulose fiber, which may lead to high ionic strength and affect the biosorption of dyes onto biomass [27]. In order to investigate the influence of inorganic salts in dye biosorption process, the experiments were carried out using 100 mL of dye solution with an initial dye concentration of 50 mg/L containing various NaCl concentrations ranging from 0 to 1.0 M.

As depicted in Fig. 1(d), the dye uptakes were enhanced by 4.04, 4.03, 3.97, 0.98, and 4.90 mg/g for raw as well as LR, PE, AM, and AP-treated biomasses, respectively, in the presence of NaCl at 0.1 M, suggesting that the chloride at relatively low concentrations could enhance the electrostatic force of biomass to dyes, thereby stimulating dye removal. Thereafter, the biosorption capabilities returned to their original levels at 0.4 M and decreased as the chloride increased from 0.5 to 1.0 M. This could be explained by the competition between chloride anions (Cl^-) (present in salt used to change the ionic strength of solution) and negatively charged Neutral Red dye species for the same binding sites on the biosorbent surface [14,28].

3.1.5. Reaction time

To determine the optimum reaction time for the Neutral Red dye removal, the raw and chemically modified biomasses (100 mg) were equilibrated with 100 mL of 50 mg/L dye solution at pH 3.0 with 2.5% (V/V) Tween 80 and 0.1 M inorganic salt NaCl, respectively. As displayed in Fig. 1(e), it is clear that

initial biosorption of dye occurred much more rapidly and the majority of dye uptake took place within the first 60 min of contact time. As a result of filling some binding sites with dye molecules, the availability of these sites and so the rate of the biosorption decreased by the time passes [12].

3.2. Biosorption isotherm studies

In the present investigation, the isotherm study of heterocycle dye Neutral Red was conducted with raw and chemically modified biomasses by changing the initial dye concentration in the range of 5–200 mg/L. The Langmuir, Freundlich, and Temkin isotherm models were used to describe the equilibrium biosorption data (Table 2).

3.2.1. Langmuir model

The Langmuir isotherm model assumes that the biosorption takes place in the monolayer form at specific homogeneous sites within the biomass, meaning that once a dye molecule occupies a site, no further biosorption can occur at this site. The linear form of the Langmuir equation is expressed as follows [29]:

$$\frac{1}{q_e} = \frac{1}{q_{\max}} + \left(\frac{1}{q_{\max} K_L} \right) \frac{1}{C_e} \quad (5)$$

where q_e and q_{\max} are the equilibrium and monolayer biosorption capabilities of the biomass (mg/g), respectively. The C_e represents the dye concentration in solution at equilibrium (mg/L), and the Langmuir constant K_L is related to the energy of biosorption (L/mg).

As shown in Table 2, it is evident from the corresponding linear regression correlation coefficient values R^2 that Langmuir model was suitable for describing the biosorption of heterocycle dye Neutral Red; further demonstrating that monolayer biosorption onto cell surface is the mechanism for the raw and chemically modified *P. subacida* biomasses to remove the dye. As a result, once an adsorbate occupies a site no further biosorption can occur at this site [29].

3.2.2. Freundlich model

The Freundlich isotherm model involves heterogeneous biosorption over the surface of the biosorbent and it can be presented by the following linearized equation [30]:

Table 2

Isotherms of the biosorption of heterocycle dye Neutral Red by raw and chemically modified biomasses from *P. subacida* in the optimal conditions

Biosorption isotherm	Biomass				
	Raw	Lipid removal	Phosphate esterification	Amine methylation	Amine propylamination
<i>Langmuir model</i>					
q_{\max} (mg/g)	58.4795	58.8235	57.1429	42.0168	75.7576
K_L (L/mg)	0.0458	0.0483	0.0452	0.0731	0.0765
R^2	0.9985	0.9975	0.9977	0.9980	0.9992
<i>Freundlich model</i>					
K_F (mg/g)	8.5122	9.7757	8.8004	11.8734	20.4054
n	2.7108	2.9317	2.8161	4.1597	3.9557
R^2	0.9346	0.9480	0.9564	0.9458	0.9582
<i>Temkin model</i>					
K_T (L/mg)	0.6256	0.7287	0.6431	2.4390	1.9175
b_T (J/mol)	221.2194	226.6462	229.0095	381.8746	200.4131
R^2	0.9895	0.9851	0.9892	0.9868	0.9802

$$\ln q_e = \ln K_F + \frac{1}{n} \ln C_e \quad (6)$$

where q_e is the equilibrium biosorption capability of the biomass (mg/g), K_F is the Freundlich constant (mg/g), and $1/n$ is the empirical parameter relating the biosorption intensity, which varies with the heterogeneity of the material. In Table 2, it is demonstrated that the Freundlich model does not fit well with the studied biosorption processes because R^2 has lower values than those in the Langmuir isotherm model.

3.2.3. Temkin model

Temkin isotherm was also applied to evaluate the experimental data. Unlike the Langmuir and Freundlich models, the Temkin isotherm model takes into consideration the interactions between biomass and dye to be adsorbed and is based on the assumption that the free energy of biosorption is a function of the surface coverage [31]:

$$q_e = \frac{RT}{b_T} \ln(K_T C_e) \quad (7)$$

where q_e is the equilibrium biosorption capability of the biomass (mg/g), b_T is the Temkin constant related to heat of biosorption (J/mol), K_T is the Temkin isotherm constant (L/mg), T is the temperature (K), and R is the ideal gas constant (8.134 J/mol·K). As demonstrated in Table 2, the highest A_T indicated a stronger interaction between the dye and the biomass surface. Since the R^2 values were less than those of Langmuir

model, the kinetic data could not be well described by the Temkin isotherm model.

3.3. Biosorption kinetic studies

Batch biosorption kinetics of heterocycle dye Neutral Red uptake was examined using the pseudo-first-order, pseudo-second-order, and intraparticle diffusion kinetic models with raw and chemically modified *P. subacida* biomasses (Fig. 2 and Table 3).

3.3.1. Pseudo-first-order model

When biosorption is processed by diffusion through a boundary, the kinetics in most cases follows the pseudo-first-order rate equation [32]:

$$\frac{dq_t}{dt} = k_1(q_e - q_t) \quad (8)$$

where q_e and q_t are the amounts of dye adsorbed (mg/g) at equilibrium and at time t (min), respectively, and k_1 is the rate constant of pseudo-first-order kinetics (min^{-1}). Integrating this for the boundary conditions $q_t = 0$ at $t = 0$ and $q_t = q_t$ at $t = t$, gives

$$\ln(q_e - q_t) = \ln q_e - k_1 t \quad (9)$$

A straight line of $\ln(q_e - q_t)$ vs. t suggests the applicability of this kinetic model and q_e and k_1 can be determined from the intercept and slope of the plot, respectively.

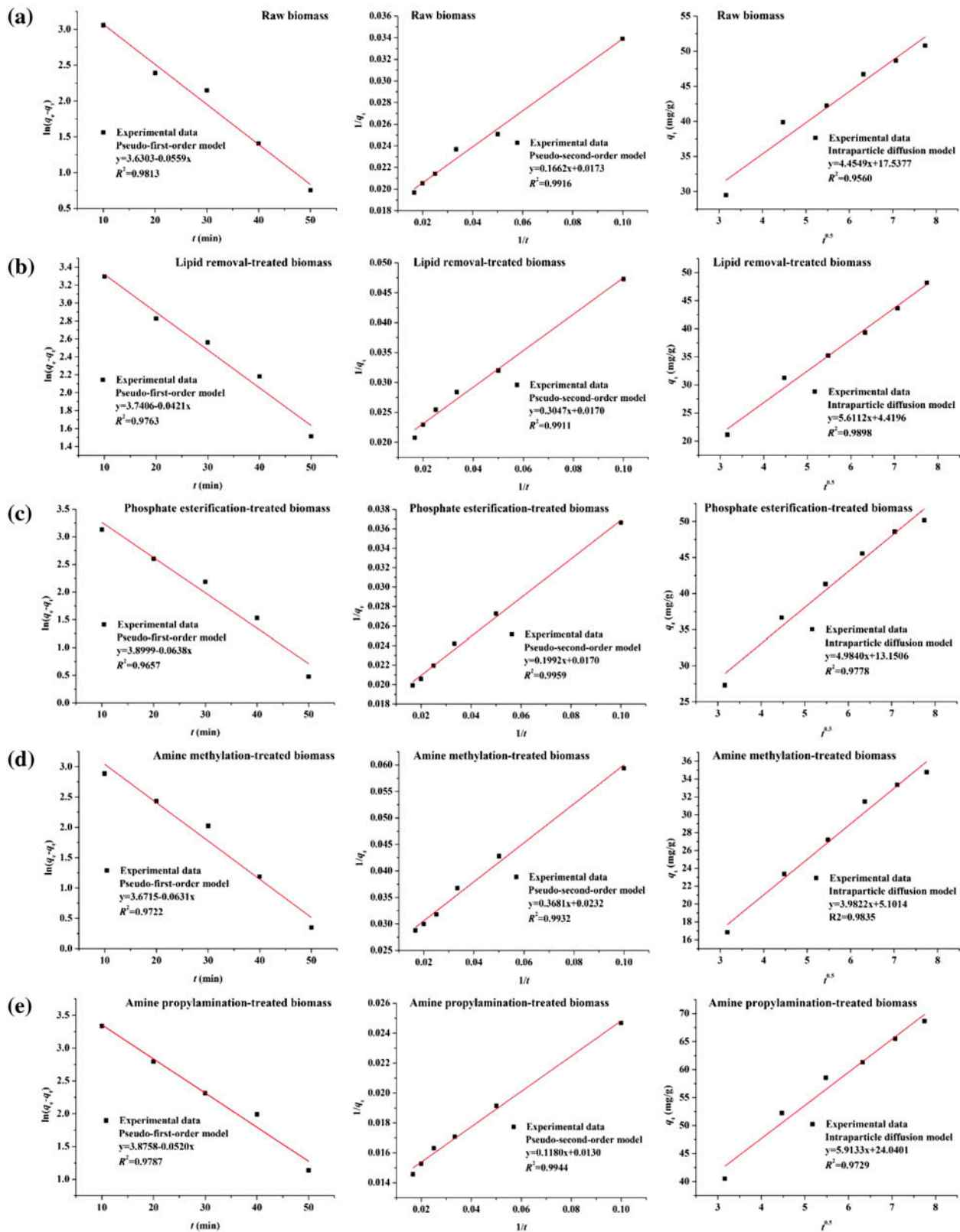


Fig. 2. Batch biosorption kinetics of (a) raw, (b) lipid removal treated, (c) PE-treated, (d) AM-treated, and (e) AP-treated *P. subacida* biomasses for heterocycle dye Neutral Red uptake.

Table 3

Kinetics parameters obtained from pseudo-first-order, pseudo-second-order and intraparticle diffusion models for the biosorption of heterocycle dye Neutral Red by raw and chemically modified biomasses from *P. subacida* in the optimal conditions

Kinetic model	Biomass				
	Raw	Lipid removal	Phosphate esterification	Amine methylation	Amine propylamination
<i>Pseudo-first-order model</i>					
k_1 (min ⁻¹)	0.0559	0.0421	0.0638	0.0631	0.0520
q_1 (mg/g)	37.7241	42.1233	49.3975	39.3108	48.2213
R^2	0.9813	0.9763	0.9657	0.9722	0.9787
<i>Pseudo-second-order model</i>					
$k_2 \times 10^{-3}$ (g/mg min)	1.8008	0.9485	1.4508	1.4622	1.4322
q_2 (mg/g)	57.8035	58.8235	58.8235	43.1034	76.9231
R^2	0.9916	0.9911	0.9959	0.9932	0.9944
<i>Intraparticle diffusion model</i>					
k_p (mg/g min ^{0.5})	4.4549	5.6112	4.9839	3.9821	5.9133
C (mg/g)	17.5380	4.4196	13.1510	5.1014	24.0400
R^2	0.9560	0.9898	0.9778	0.9835	0.9729

It is worth noting that the experimental q_e must be known for the application of this model [33,34]. According to the pseudo-first-order constants and R^2 values, it can be obviously seen that the calculated $q_{e\text{ cel}}$ values were not in good agreement with the experimental data of $q_{e\text{ exp}}$ and the constants k_1 of pseudo-first-order model were found in the range from 0.0421 to 0.0638, which were relatively low. As shown in Fig. 2, there was a deviation from the straight line of $\ln(q_e - q_t)$ vs. t after the first 60 min for raw and chemically modified biomasses, indicating that the pseudo-first-order model could not explain the Neutral Red dye removal process adequately [35].

3.3.2. Pseudo-second-order model

The pseudo-second-order model is based on a certain assumption that the rate-limiting step is chemical sorption or chemisorption involving valance forces through sharing or exchange of electrons between adsorbent and adsorbate as covalent forces [36]. The model may be expressed as [31]:

$$\frac{dq_t}{dt} = k_2(q_e - q_t)^2 \quad (10)$$

where k_2 is the rate constant for the pseudo-second-order kinetics (g/mg·min); q_e (mg/g) is the maximum biosorption capacity; and q_t (mg/g) is the amount of dye adsorbed at time t (min). Separating the variables in Eq. (10) gives:

$$\frac{dq_t}{(q_e - q_t)^2} = k_2 dt \quad (11)$$

Integrating this for the boundary conditions $q_t = 0$ at $t = 0$ and $q_t = q_t$ at $t = t$, gives

$$\frac{1}{(q_e - q_t)^2} = \frac{1}{q_e} + k_2 t \quad (12)$$

which is the integrated rate law for a pseudo-second-order reaction. Eq. (12) can be rearranged to obtain:

$$q_t = \frac{1}{(1/k_2 q_e^2) + (t/q_e)} \quad (13)$$

which has a linear form of:

$$\frac{1}{q_t} = \frac{1}{t k_2 q_e^2} + \frac{1}{q_e} \quad (14)$$

If pseudo-second-order kinetics is applicable, the plot of $1/q_t$ against $1/t$ should give a straight, from which q_e and k_2 can be obtained from the slope and intercept of the plot, respectively [34,37]. Fig. 2 depicts the pseudo-second-order plots for biosorption of heterocycle dye Neutral Red onto raw and all-treated *P. subacida* biomasses. The pseudo-second-order rate constants k_2 , the calculated q_e values, and the corresponding linear regression correlation coefficient values R^2 are given in Table 3. From Table 3, it was

noticed that the R^2 values of pseudo-second-order model exceeded 0.99 and the $q_{e\text{ cal}}$ calculated from pseudo-second-order model were more consistent with the experimental $q_{e\text{ exp}}$ than those calculated from the pseudo-first-order model. Thus, the results suggested that the pseudo-second-order mechanism is predominant for the biosorption of Neutral Red dye onto raw and modified *P. subacida* biomasses, and it is considered that the overall rate of the dye biosorption process appeared to be controlled by the chemisorption process [38,39].

3.3.3. Intraparticle diffusion model

To establish the exact diffusion mechanism and to determine the rate-limiting step, the biosorption kinetic data were further processed. In general, any dye adsorption process involves the following four main successive transport steps which are (i) migration of dye molecules through bulk of the solution to the adsorbent surface (bulk diffusion); (ii) transport of dye molecules from the boundary layer to the surface of adsorbent (film diffusion); (iii) diffusion of dye molecules from the surface to the interior pores of particle (intraparticle diffusion or pore diffusion); (iv) adsorption of dye molecules at an active site on the material surface (chemical reaction via ion-exchange, complexation and/or chelation) [40].

Since the particles are vigorously agitated during the biosorption period, it is assumed that the rate is not limited by mass transfer from bulk of the solution to the particle external surface [35]. Weber and Morris stated that if intraparticle diffusion is the rate-controlling factor, uptake of the adsorbate varies with the square root of time [41]. Hence, rates of adsorption are usually measured by determining the biosorption capacity of the adsorbent as a function of the square root of time [42]. The intraparticle diffusion model equation can be written as [41]:

$$q_t = k_p t^{1/2} + C \quad (15)$$

where q_t (mg/g) is the amount of dye adsorbed at time t (min), C is the intercept, and k_p is the intraparticle diffusion rate constant ($\text{mg/g min}^{0.5}$), which can be evaluated from the slope of the linear plot of uptake, q_t , vs. the square root of time ($t^{0.5}$) (Fig. 2 and Table 3). Based on this model, the plot of q_t vs. $t^{0.5}$ should result in a linear relationship if intraparticle diffusion is involved in the adsorption process and if these lines pass through the origin then intraparticle diffusion is the rate-controlling step. When the plots do not pass through the origin, this is indicative of some degree of

boundary layer control which further demonstrates that the intraparticle diffusion is not the only rate-controlling step, but other processes are also controlling the rate of adsorption, all of which may be operating simultaneously [43]. As displayed in Fig. 2, the lines do not pass through the origin indicating that the intraparticle diffusion model is not the only rate-limiting mechanism. Therefore, it can be concluded that biosorption of heterocycle dye Neutral Red onto raw and chemically modified *P. subacida* biomasses is a complex process and both intraparticle diffusion and surface biosorption contribute to the rate-limiting step [44]. Moreover, the values of intercept give an idea about the boundary layer thickness such as the larger the intercept, the greater the boundary layer effect [35].

3.4. Thermodynamic analysis of biosorption process

The influence of temperature on the biosorption capabilities was studied by carrying out a series of experiments at 28, 38, and 48 °C for all the systems. It is observed that the biosorption amounts decreased from 53.16 to 49.48 mg/g, 51.24 to 47.65 mg/g, 56.62 to 52.85 mg/g, 37.56 to 34.74 mg/g, and 71.64 to 67.05 mg/g for raw, LR, PE, AM and AP-treated biomasses, respectively, as the reaction temperature increased from 28 °C to 48 °C, indicating that the biosorption process is exothermic in nature. The decrease in the equilibrium biosorption of dyes with increase in temperature suggested that the dyes biosorption onto biomass is favorable at relatively lower temperature.

To evaluate the thermodynamic feasibility and to confirm the nature of the dye removal process by raw and chemically modified biomasses, thermodynamic parameters such as changes in Gibbs free energy (ΔG°), enthalpy (ΔH°), and entropy (ΔS°) were determined using Eqs. (16) and (17).

$$\ln K_L = \frac{\Delta S^\circ}{R} - \frac{\Delta H^\circ}{RT} \quad (16)$$

$$\Delta G^\circ = \Delta H^\circ - T\Delta S^\circ \quad (17)$$

where R is the universal gas constant (8.314 J/mol·K), T is the temperature (K), and K_L is the Langmuir constant (L/mg) obtained from the plot of $1/q_e$ vs. $1/C_e$. The estimated data are presented in Table 4. The negative values of ΔH° changes suggested the exothermic nature of the biosorption process, so raising temperature leads to a lower affinity and weak dye binding potential at equilibrium. The negative values of ΔS° changes described the decrease in randomness at the adsorbent–solution interface during the biosorption,

Table 4

Thermodynamic parameters for the biosorption of heterocycle dye Neutral Red by raw and chemically modified biomasses from *P. subacida*

Biomass	ΔH° (kJ/mol)	ΔS° (J/mol·K)	ΔG° (kJ/mol)		
			28°C	38°C	48°C
Raw	-7.6128	-4.6561	-6.2113	-6.1648	-6.1182
Lipid removal	-7.8914	-5.0670	-6.3663	-6.3156	-6.2649
Phosphate esterification	-7.4694	-4.8319	-6.0150	-5.9667	-5.9184
Amine methylation	-5.8363	-5.4916	-4.1833	-4.1284	-4.0735
Amine propylamination	-9.5469	-3.7427	-8.4204	-8.3829	-8.3455

indicating that Neutral Red dye is more stable on the biomass surface. Moreover, the negative values of ΔG° changes demonstrated that the biosorption process is spontaneous in nature.

3.5. Characterization of biosorption

The results of the present study showed that blocking of amine groups by methylation dramatically decreased the biosorption of heterocycle dye Neutral Red, indicating that especially amine functional group plays an important role during this process. To further evaluate the possible dye–biosorbent interactions, the raw and chemically modified *P. subacida* biomasses before and after dye biosorption were characterized by FT-IR, SEM, and X-ray diffraction, respectively.

3.5.1. FT-IR analysis

A FT-IR examination of the adsorbent surface before and after dye biosorption reaction possibly provides information regarding the surface groups or the surface site(s) where the biosorption has taken place [45]. In this study, the spectra of raw and chemically modified *P. subacida* biomasses before and after dye loading are shown in Fig. 3 representing the complex nature of the adsorbent.

In the raw *P. subacida* biomass, the broad and strong vibration around 3,000–3,600 cm^{-1} is indicative of the presence of –OH and –NH groups on fungal biomass. The peak at 2,922.59 cm^{-1} is due to the asymmetric and symmetric –CH stretching of aliphatic groups. The strong peaks at 1,646.84 and 1,538.25 cm^{-1} are attributed to the stretching vibration of –NH, carboxyl (–C=O), or –C=N (amide I and II) groups. A peak at 1,453.84 cm^{-1} is due to the –CH bending vibrations. The band observed at 994.89 cm^{-1} is assigned to the –C–O stretching vibration of alcohols and carboxylic acids. Comparison of dye-loaded biomass with FT-IR spectrum of pure biomass displayed

significant changes in some of the peaks. As can be seen in Fig. 3(a), the shift and reduction in the peak at 3,246.55 cm^{-1} suggest the major role of –OH and –NH groups for biosorption of Neutral Red dye onto fungal biomass. Furthermore, the obvious decline in the peak at 1,621.15 cm^{-1} reflects the effect of carboxyl groups on the binding of Neutral Red dye. The band at 994.89 cm^{-1} was remarkably shifted to 1,022.10 cm^{-1} after dye biosorption, indicating the strong interactions of the dye molecules with carboxylic acid functional groups of the biomass surface.

In the lipid removal-treated *P. subacida* biomass, the bands observed at 1,632.42 and 1,338.50 cm^{-1} shifting to 1,647.63 and 1,315.37 cm^{-1} indicate that the –CH bending, –CH₃ stretch, or –COO symmetric stretch of carboxylic acids on treated fungal biomass play a key role in biosorption of heterocycle dye Neutral Red (Fig. 3(b)). In Fig. 3(c) it is demonstrated that the FT-IR spectrum of the PE-treated *P. subacida* biomass exposed to Neutral Red dye displayed a new peak at 1,455.06 cm^{-1} , which is due to the –CH deformations of –CH₂ or –CH₃ groups in aliphatics. The spectrum also exhibited the intensity increase in the adsorption peak from 1,361.81 to 1,372.68 cm^{-1} , corresponding to the –CH bending vibration of carboxylic acids.

In the AM-treated *P. subacida* biomass, there was a significant shift and reduction at peak 3,311.93–3,281.44 cm^{-1} . This may be explained by the blockage of –NH functional groups to the biomass surface following modification with methanal and methanoic acid. The peak at 2,360.54 cm^{-1} remained unchanged. The strong peak at 1,638.92 cm^{-1} was shifted to 1,649.16 cm^{-1} , which can be attributed to a –C=O or –C–O stretching vibration of carboxylic acids. Shifting and intensification of a strong peak from 1,307.12 to 1,315.26 cm^{-1} is relative to a –C–N stretch of amide or amine (Fig. 3(d)). While in the case of AP-treated *P. subacida* biomass, an apparent reduction in the adsorption peak from 3,445.03 to 3,420.78 cm^{-1} was observed, which is ascribed to the presence and high interaction of –NH and –OH groups on fungal biomass with

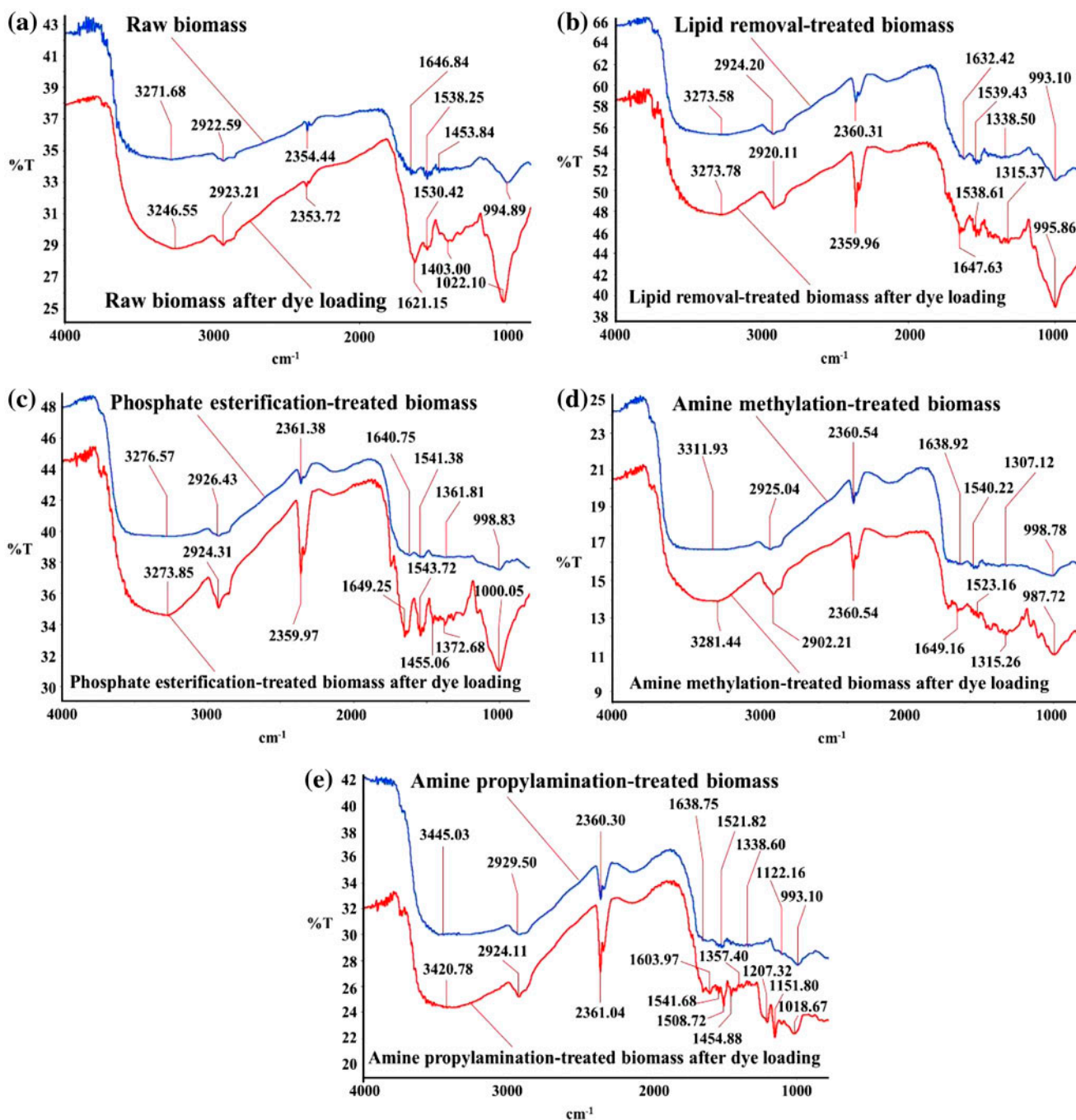


Fig. 3. FT-IR spectra of (a) raw, (b) lipid removal treated, (c) PE-treated, (d) AM-treated, and (e) AP-treated *P. subacida* biomasses before and after dye biosorption.

Neutral Red dye. Additionally, the broad and strong vibration around 900–1,650 cm^{-1} in FT-IR spectra of the propylaminated biomass after dye loading is more significant than that in the other chemically modified fungal biomasses. A sharp peak at 1,638.75 cm^{-1} was significantly shifted to 1,603.97 cm^{-1} , indicating the

effect of $-\text{C}=\text{O}$ groups in the biosorption process. It is also noteworthy that several new peaks at 1,508.72, 1,454.88, and 1,207.32 cm^{-1} for modified biomass appeared, which may be due to the role of the asymmetric and symmetric $-\text{CH}$ stretching of aliphatic groups in biosorption of Neutral Red dye (Fig. 3(e)).

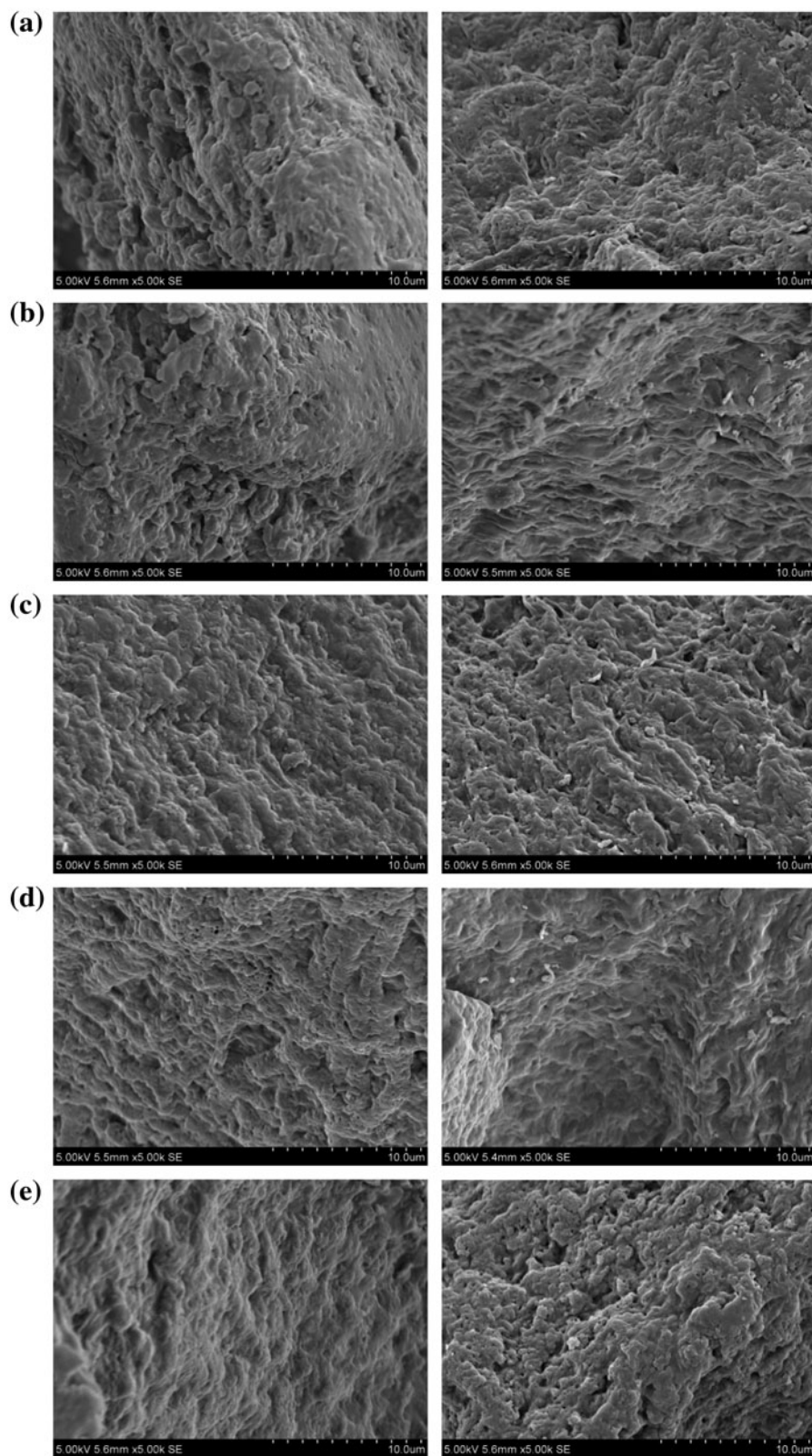


Fig. 4. SEM photomicrographs of (a) raw, (b) lipid removal treated, (c) PE-treated, (d) AM-treated, and (e) AP-treated *P. subacida* biomasses before and after dye biosorption.

These observations indicate that several functional groups on the cell surface of the *P. subacida* biomass are responsible for binding of Neutral Red dye ions during the biosorption process. Moreover,

different biosorption capabilities of heterocycle dye Neutral Red may be attributed to different interactions among dye molecules and fungal biomasses [21].

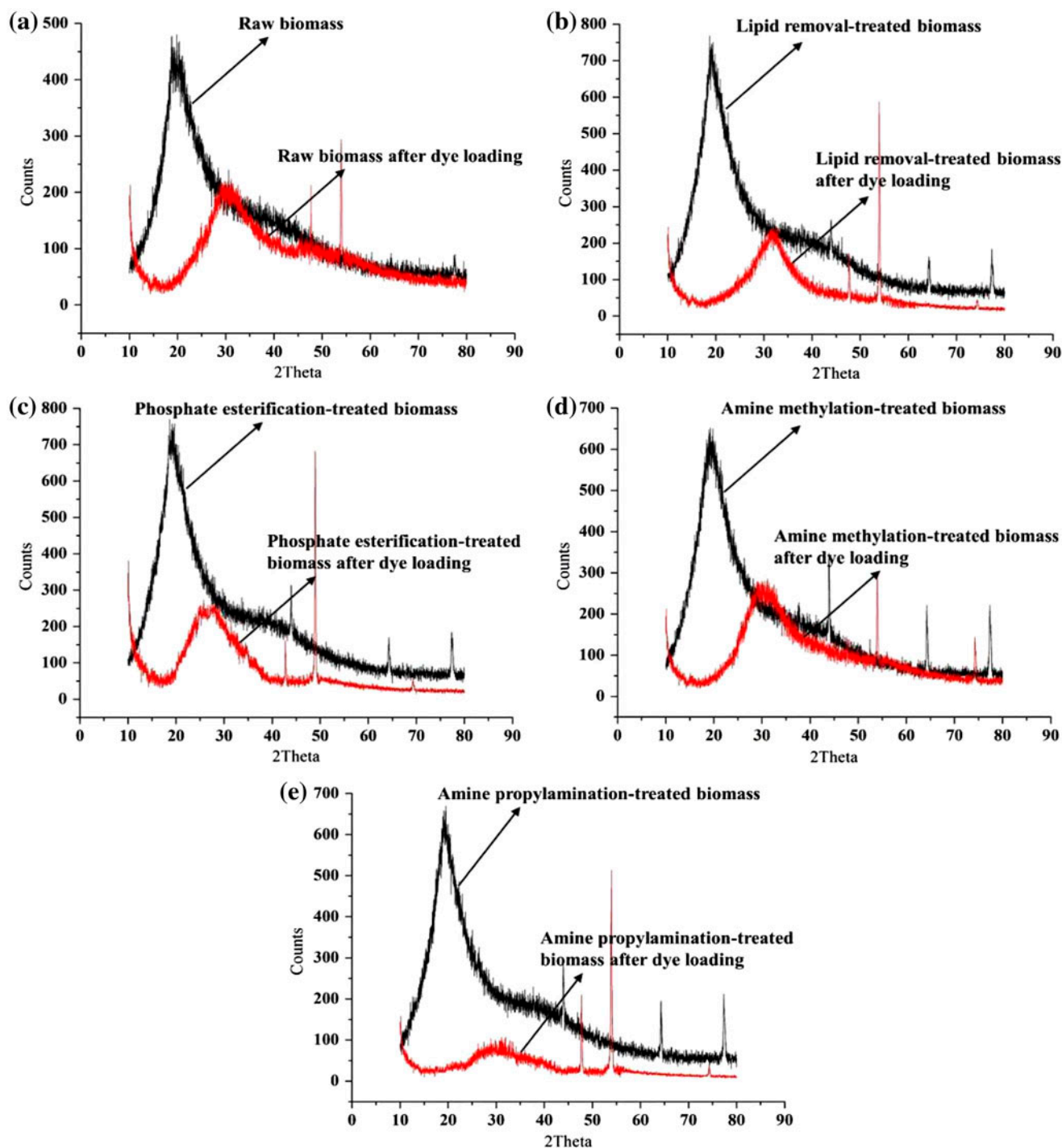


Fig. 5. X-ray diffractograms of (a) raw, (b) lipid removal treated, (c) PE-treated, (d) AM-treated, and (e) AP-treated *P. subacida* biomasses before and after dye biosorption.

3.5.2. SEM analysis

SEM has been proved as a primary and effective tool for characterizing the surface morphology of the adsorbent [3]. As can be seen from Fig. 4, SEM photomicrographs of raw and chemically modified *P. subacida* biomasses obtained before and after Neutral Red dye loading indicated surface alterations in the biosorbent after biosorption. Porous nature of the biomass before dye biosorption with a grooved structure is clearly visible in the SEM photomicrograph. The large surface area of the biosorbent is thus ideal for binding the solute. After occupied by Neutral Red dye, biomass pores were not visible.

3.5.3. XRD study

Crystalline nature of the compounds was determined through an efficient technique known as X-ray diffraction [45]. In this analysis, sharp and well-defined peaks were obtained for crystalline substance and diffused peaks were observed for amorphous compound. As shown in Fig. 5, the XRD patterns of raw and chemically modified *P. subacida* biomasses indicate shapes of typical crystalline in nature and show sharp peaks corresponding to $2\theta = 19.88, 19.36, 19.62, 19.26,$ and $19.50,$ respectively. On the contrary, the XRD patterns of the biomasses after dye loading demonstrate that the sharp peaks changed into diffused ones and the crystalline nature of biomass changed into amorphous one, but some crystalline zones were still observed. It is suggested that the structure of *P. subacida* biomass was modified with coverage of dyes during the biosorption process.

4. Conclusions

P. subacida biomass was modified with chemical methods by a simple procedure and the biosorption properties of these modified biomasses for heterocycle dye Neutral Red were characterized. The results showed that the developed biomasses exhibited good potentials for dye biosorption process. Dye uptake was dependent on initial pH, initial dye concentration, surfactant Tween 80, ionic strength, and reaction time. Kinetic and equilibrium data were explained adequately by the pseudo-second-order kinetics and Langmuir isotherm model, further suggesting that monolayer biosorption onto cell surface is the mechanism for the *P. subacida* biomass to remove dye molecules. Negative values of ΔH° and ΔG° indicated that the biosorption process is spontaneous, feasible, and exothermic in nature. Additionally, propylaminated treatment obviously increased the biosorption perfor-

mances of the biomass, implying that amine functional groups play a major role in this process at optimum pH. As a conclusion, the suggested biomass may be an alternative to existing costly biosorbent material for heterocycle dye removal.

Acknowledgments

We express our gratitude to Dr Hai-Jiao Li (Chinese Center for Disease Control and Prevention, China) and Dr Feng Peng (Beijing Forestry University, China) for improving the manuscript. This study was supported by the Fundamental Research Funds for the Central Universities (Nos. BLX2014-36, JC2013-1) and the National Natural Science Foundation of China (Project No. 31422001).

References

- [1] Q.H. Hu, Z.P. Xu, S.Z. Qiao, F. Haghseresht, M. Wilson, G.Q. Lu, A novel color removal adsorbent from heterocoagulation of cationic and anionic clays, *J. Colloid Interface Sci.* 308 (2007) 191–199.
- [2] K.Z. Elwakeel, Removal of Reactive Black 5 from aqueous solutions using magnetic chitosan resins, *J. Hazard. Mater.* 167 (2009) 383–392.
- [3] G.L. Dotto, L.A.A. Pinto, Adsorption of food dyes onto chitosan: Optimization process and kinetic, *Carbohydr. Polym.* 84 (2011) 231–238.
- [4] T. Akar, İlknur Tosun, Z. Kaynak, E. Kavas, G. Incirkus, S.T. Akar, Assessment of the biosorption characteristics of a macro-fungus for the decolorization of Acid Red 44 (AR44) dye, *J. Hazard. Mater.* 171 (2009) 865–871.
- [5] Z. Aksu, Application of biosorption for the removal of organic pollutants: A review, *Process Biochem.* 40 (2005) 997–1026.
- [6] Č. Novotný, K. Svobodová, A. Kasinath, P. Erbanová, Biodegradation of synthetic dyes by *Irpex lacteus* under various growth conditions, *Int. Biodeterior. Biodegrad.* 54 (2004) 215–223.
- [7] X.J. Xiong, X.J. Meng, T.L. Zheng, Biosorption of C.I. Direct Blue 199 from aqueous solution by nonviable *Aspergillus niger*, *J. Hazard. Mater.* 175 (2010) 241–246.
- [8] S. Mona, A. Kaushik, C.P. Kaushik, Biosorption of reactive dye by waste biomass of *Nostoc linckia*, *Ecol. Eng.* 37 (2011) 1589–1594.
- [9] Y. Safa, H.N. Bhatti, Adsorptive removal of direct textile dyes by low cost agricultural waste: Application of factorial design analysis, *Chem. Eng. J.* 167 (2011) 35–41.
- [10] G. Bayramoğlu, G. Çelik, M.Y. Arica, Biosorption of Reactive Blue 4 dye by native and treated fungus *Phanerocheate chrysosporium*: Batch and continuous flow system studies, *J. Hazard. Mater.* 137 (2006) 1689–1697.
- [11] T. Akar, M. Divriklioglu, Biosorption applications of modified fungal biomass for decolorization of Reactive Red 2 contaminated solutions: Batch and dynamic flow mode studies, *Bioresour. Technol.* 101 (2010) 7271–7277.

- [12] L.N. Du, B. Wang, G. Li, S. Wang, D.E. Crowley, Y.H. Zhao, Biosorption of the metal-complex dye Acid Black 172 by live and heat-treated biomass of *Pseudomonas* sp. strain DY1: Kinetics and sorption mechanisms, *J. Hazard. Mater.* 205–206 (2012) 47–54.
- [13] M.X. Loukidou, K.A. Matis, A.I. Zouboulis, M. Liakopoulou-Kyriakidou, Removal of As(V) from wastewaters by chemically modified fungal biomass, *Water Res.* 37 (2003) 4544–4552.
- [14] Z. Aksu, E. Balibek, Effect of salinity on metal-complex dye biosorption by *Rhizopus arrhizus*, *J. Environ. Manage.* 91 (2010) 1546–1555.
- [15] Y.C. Dai, Polypore diversity in China with an annotated checklist of Chinese polypores, *Mycoscience* 53 (2012) 49–80.
- [16] Y.C. Dai, B.K. Cui, H.S. Yuan, B.D. Li, Pathogenic wood-decaying fungi in China, *Forest Pathol.* 37 (2007) 105–120.
- [17] Y.C. Dai, Z.L. Yang, B.K. Cui, C.J. Yu, L.W. Zhou, Species diversity and utilization of medicinal mushrooms and fungi in china (Review), *Int. J. Med. Mushrooms* 11 (2009) 287–302.
- [18] J. Si, X.C. Li, B.K. Cui, Decolorization of heterocycle dye Neutral Red by white-rot fungus *Perenniporia subacida*, *Desalin. Water Treat.* 52 (2014) 5594–5604.
- [19] C. Yenikaya, E. Atar, A. Olgun, N. Atar, S. İlhan, F. Çolak, Biosorption study of anionic dyes from aqueous solutions using *Bacillus amyloliquefaciens*, *Eng. Life Sci.* 10 (2010) 233–241.
- [20] M.S. Chiou, G.S. Chuang, Competitive adsorption of dye metanil yellow and RB15 in acid solutions on chemically cross-linked chitosan beads, *Chemosphere* 62 (2006) 731–740.
- [21] M. Kousha, E. Daneshvar, M.S. Sohrabi, M. Jokar, A. Bhatnagar, Adsorption of acid orange II dye by raw and chemically modified brown macroalga *Stoecospherum marginatum*, *Chem. Eng. J.* 192 (2012) 67–76.
- [22] P.D. Shah, S.R. Dave, M.S. Rao, Enzymatic degradation of textile dye Reactive Orange 13 by newly isolated bacterial strain *Alcaligenes faecalis* PMS-1, *Int. Biodeterior. Biodegrad.* 69 (2012) 41–50.
- [23] F. Çolak, N. Atar, A. Olgun, Biosorption of acidic dyes from aqueous solution by *Paenibacillus macerans*: Kinetic, thermodynamic and equilibrium studies, *Chem. Eng. J.* 150 (2009) 122–130.
- [24] G.M.L. Ruiz-Aguilar, J.M. Fernández-Sánchez, R. Rodríguez-Vázquez, H. Poggi-Varaldo, Degradation by white-rot fungi of high concentrations of PCB extracted from a contaminated soil, *Adv. Environ. Res.* 6 (2002) 559–568.
- [25] T. Eriksson, J. Börjesson, F. Tjerneld, Mechanism of surfactant effect in enzymatic hydrolysis of lignocellulose, *Enzyme Microb. Technol.* 31 (2002) 353–364.
- [26] J. Zhou, W.Y. Jiang, J. Ding, X.D. Zhang, S.X. Gao, Effect of Tween 80 and β -cyclodextrin on degradation of decabromodiphenyl ether (BDE-209) by white rot fungi, *Chemosphere* 70 (2007) 172–177.
- [27] C.M. Carliell, S.J. Barclay, C. Shaw, A.D. Wheatley, C.A. Buckley, The effect of salts used in textile dyeing on microbial decolourisation of a reactive azo dye, *Environ. Technol.* 19 (1998) 1133–1137.
- [28] N.S. Maurya, A.K. Mittal, P. Cornel, E. Rother, Biosorption of dyes using dead macro fungi: Effect of dye structure, ionic strength and pH, *Bioresour. Technol.* 97 (2006) 512–521.
- [29] I. Langmuir, The adsorption of gases on plane surfaces of glass, mica and platinum, *J. Am. Chem. Soc.* 40 (1918) 1361–1403.
- [30] H.M.F. Freundlich, Über die adsorption in lösungen, *Z. Phys. Chem.* 57 (1906) 385–470.
- [31] Y.S. Ho, G. McKay, Sorption of dye from aqueous solution by peat, *Chem. Eng. J.* 70 (1998) 115–124.
- [32] S. Lagergren, Zur theorie der sogenannten adsorption gelöster stoffe (About the theory of so-called adsorption of soluble substances), *Kungliga Svenska Vetenskapsakademiens Handlingar* 24 (1898) 1–39.
- [33] H.B. Senturk, D. Ozdes, C. Duran, Biosorption of Rhodamine 6G from aqueous solutions onto almond shell (*Prunus dulcis*) as a low cost biosorbent, *Desalination* 252 (2010) 81–87.
- [34] G. Crini, P.M. Badot, Application of chitosan, a natural aminopolysaccharide, for dye removal from aqueous solutions by adsorption processes using batch studies: A review of recent literature, *Prog. Polym. Sci.* 33 (2008) 399–447.
- [35] B.H. Hameed, Equilibrium and kinetic studies of methyl violet sorption by agricultural waste, *J. Hazard. Mater.* 154 (2008) 204–212.
- [36] S.S. Sen Gupta, K.G. Bhattacharyya, Kinetics of adsorption of metal ions on inorganic materials: A review, *Adv. Colloid Interface Sci.* 162 (2011) 39–58.
- [37] M. Doğan, M. Alkan, Ö. Demirbaş, Y. Özdemir, C. Özmetin, Adsorption kinetics of maxilon blue GRL onto sepiolite from aqueous solutions, *Chem. Eng. J.* 124 (2006) 89–101.
- [38] R. Ahmad, R. Kumar, Adsorption of amaranth dye onto alumina reinforced polystyrene, *Clean Soil, Air, Water* 39 (2011) 74–82.
- [39] V.K. Gupta, A. Mittal, V. Gajbe, J. Mittal, Removal and Recovery of the hazardous azo dye acid orange 7 through adsorption over waste materials: Bottom ash and de-oiled soya, *Ind. Eng. Chem. Res.* 45 (2006) 1446–1453.
- [40] G. Crini, H.N. Peindy, F. Gimbert, C. Robert, Removal of C.I. Basic Green 4 (Malachite Green) from aqueous solutions by adsorption using cyclodextrin-based adsorbent: Kinetic and equilibrium studies, *Sep. Purif. Technol.* 53 (2007) 97–110.
- [41] W.J. Weber, J.C. Morris, Kinetics of adsorption on carbon from solution, *J. Sanit. Eng. Div. ASCE* 89 (1963) 31–59.
- [42] Y.S. Ho, G. McKay, Sorption of dyes and copper ions onto biosorbents, *Process Biochem.* 38 (2003) 1047–1061.
- [43] S.M. Maliyekkal, S. Shukla, L. Philip, I.M. Nambi, Enhanced fluoride removal from drinking water by magnesia-amended activated alumina granules, *Chem. Eng. J.* 140 (2008) 183–192.
- [44] E. Bulut, M. Özacar, İ.A. Şengil, Adsorption of malachite green onto bentonite: Equilibrium and kinetic studies and process design, *Microporous Mesoporous Mater.* 115 (2008) 234–246.
- [45] C. Namasivayam, D. Kavitha, IR, XRD and SEM studies on the mechanism of adsorption of dyes and phenols by coir pith carbon from aqueous phase, *Microchem. J.* 82 (2006) 43–48.